The scattering of electromagnetic radiation from dielectric scatterers

1977 J. Phys. A: Math. Gen. 10 413

(http://iopscience.iop.org/0305-4470/10/3/014)

J. Phys. A: Math. Gen., Vol. 10, No. 3, 1977. Printed in Great Britain.

The scattering of electromagnetic radiation from dielectric scatterers

N K Uzunoglu† and A R Holt‡

† Department of Electrical Engineering, University of Essex, Wivenhoe Park, Colchester CO4 3SQ, UK

‡ Department of Mathematics, University of Essex, Wivenhoe Park, Colchester CO4 3SQ, UK

Received 15 October 1976

Abstract. The problem of electromagnetic wave scattering from arbitrarily shaped scatterers recently solved by using an integral equation formulation is extended to treat the case of scattering by infinite cylinders. The method is based on describing the internal field of the scatterer in terms of an independent set of plane wave functions. Numerical stability conditions are satisfied. Numerical results are presented for cylinders of elliptic cross section for two independent incident waves. Results are also given for scattering by three-dimensional spheroidal scatterers of refractive index $n_0 = 1{\cdot}33$. The solution presented is applicable for scatterers with size parameter $(k_0 a)$ from the Rayleigh region $(k_0 a \ll 1)$ up to the geometrical optics limit $(k_0 a \gg 1)$ provided for each given scatterer certain matrix elements can be calculated.

1. Introduction

The problem of the scattering of electromagnetic radiation from a homogeneous spherical dielectric scatterer has been solved by Mie (1908). For scatterers which are infinite rods of circular cross section, the same problem was solved by Rayleigh (1881) and Ignatowsky (1905).

For inhomogeneous scatterers, and for homogeneous scatterers of other shapes, the scattering problem cannot be solved by the classical separation of variables technique. Several approximate methods have been devised in an attempt to solve these problems. For example there are the approximations of Rayleigh (1899), Rayleigh–Gans (Gans 1912) and Stevenson (1953). However, the range of validity of these approximations is restricted to scatterers of refractive index close to that of the surrounding medium, and whose size is small compared to the wavelength of the incident radiation.

In recent years in many practical applications, knowledge of the scattering by non-spherical objects is required, and hence a general method is needed for the solution of this problem. Several attempts have been made; for example by Waterman (1965), Barber and Yeh (1975), Nelson and Eyges (1976) and Asano and Yamamoto (1975). The work of Nelson and Eyges was restricted to infinite cylinders, and that of Asano and Yamamoto sought to use spheroidal wavefunctions to solve the problem of scattering by a spheroid.

Recently we have presented a new general method which involves the solution of the integral equation formulation of the scattering problem (Uzunoglu *et al* 1976a, b,

Holt *et al* 1967a, b). The method can be applied not only to non-spherical scatterers, but to inhomogeneous scatterers also; the real restriction is involved in the necessity of being able to calculate certain matrix elements. The method guarantees that the scattering amplitude satisfies the Schwinger variational principle, and this results in numerical stability. So far the applications have been concerned with the scattering of electromagnetic radiation by spheroidal and ellipsoidal raindrops, where the refractive index is large. In this paper we consider in detail scattering by infinite cylinders of elliptic cross section. We also give results for a wide range of spheroidal scatterers of refractive index 1·33+i0·0.

2. General theory

We restrict ourselves to giving a resumé of the theory as it applies to scattering in two dimensions. An exposition of the general theory and its application to three-dimensional ellipsoids/spheroids has been given by Holt, Uzunoglu and Evans (Holt *et al* 1976a, to be referred to as I).

We shall assume that the incident wave is perpendicular to the axis ($\hat{\boldsymbol{z}}$) of the infinite cylinder. If the incident polarization is parallel to $\hat{\boldsymbol{z}}$, the incident wave will be termed an E wave. If, on the other hand, the magnetic field is parallel to $\hat{\boldsymbol{z}}$, the incident wave will be called an H wave.

For an infinitely long cylindrical scatterer of dielectric $\epsilon(\boldsymbol{\rho})$ and cross-sectional area S, the integral equation describing the scattering can be written as

$$\boldsymbol{E}(\boldsymbol{\rho}) = \boldsymbol{E}_0(\boldsymbol{\rho}) + k_0^2 \int_S \gamma(\boldsymbol{\rho}') \left(\mathbf{1} + \frac{1}{k_0^2}\boldsymbol{\nabla}\boldsymbol{\nabla}\right) g(\boldsymbol{\rho}, \boldsymbol{\rho}') \cdot \boldsymbol{E}(\boldsymbol{\rho}')\, \mathrm{d}\boldsymbol{\rho}' \tag{1}$$

where

$$\boldsymbol{E}_0(\boldsymbol{\rho}) = \hat{\boldsymbol{e}}_\mathrm{i} \exp(\mathrm{i}\boldsymbol{k}_\mathrm{i} \cdot \boldsymbol{\rho}) \tag{2}$$

is the incident wave, $\boldsymbol{k}_\mathrm{i} = k_0 (\cos\phi_\mathrm{i}, \sin\phi_\mathrm{i})$ is the incident wavevector,

$$\gamma(\boldsymbol{\rho}) = \epsilon(\boldsymbol{\rho}) - 1 \tag{3}$$

and

$$g(\boldsymbol{\rho}, \boldsymbol{\rho}') = \tfrac{1}{4}\mathrm{i} H_0^{(1)}(k_0 |\boldsymbol{\rho} - \boldsymbol{\rho}'|) \tag{4}$$

where $H_n^{(1)}(x)$ is the Hankel function of order n.

For the E-wave case, equation (1) simplifies to the scalar equation

$$E(\boldsymbol{\rho}) = \exp(\mathrm{i}\boldsymbol{k}_\mathrm{i} \cdot \boldsymbol{\rho}) + k_0^2 \int_S \gamma(\boldsymbol{\rho}') g(\boldsymbol{\rho}, \boldsymbol{\rho}') E(\boldsymbol{\rho}')\, \mathrm{d}\boldsymbol{\rho}'. \tag{5}$$

The quantity most of interest in scattering problems is the scattering amplitude which describes the far-field behaviour of the scattered field. The asymptotic form of equation (1) is defined as

$$\boldsymbol{E}(\boldsymbol{\rho}) \sim \hat{\boldsymbol{e}}_\mathrm{i} \exp(\mathrm{i}\boldsymbol{k}_\mathrm{i} \cdot \boldsymbol{\rho}) + f(\phi_\mathrm{s}) \frac{\exp(\mathrm{i}k_0\rho)}{\rho^{1/2}}; \tag{6}$$

similarly for equation (5) we have

$$E(\boldsymbol{\rho}) \sim \exp(\mathrm{i}\boldsymbol{k}_\mathrm{i} \cdot \boldsymbol{\rho}) + f(\phi_s) \frac{\exp(\mathrm{i}k_0\rho)}{\rho^{1/2}}. \tag{7}$$

Thus the scattering amplitudes for the E, H incident waves are, respectively

$$f^{(E)}(\phi_s) = \lambda \int_S \gamma(\boldsymbol{\rho}) \exp(-i\boldsymbol{\rho} \cdot \boldsymbol{k}_s) E(\boldsymbol{\rho})\, d\boldsymbol{\rho} \tag{8}$$

and

$$\boldsymbol{f}^{(H)}(\phi_s) = \lambda (\mathbf{1} - \hat{\boldsymbol{k}}_s \hat{\boldsymbol{k}}_s) \cdot \int_S \gamma(\boldsymbol{\rho}) \exp(-i\boldsymbol{\rho} \cdot \boldsymbol{k}_s) \boldsymbol{E}(\boldsymbol{\rho})\, d\boldsymbol{\rho} \tag{9}$$

where

$$\lambda = (1+i) k_0^{3/2} / 4\pi^{1/2} \tag{10}$$

and $\hat{\boldsymbol{k}}_s$ is the scattered direction given as

$$\boldsymbol{k}_s = k_0 \hat{\boldsymbol{k}}_s = k_0(\cos \phi_s, \sin \phi_s).$$

In order to solve the scattering problem only the scattered field inside the scatterer is needed—the integrations in (8) and (9) only involve the internal field. Moreover the external field, if required, can be obtained by substituting the internal field in equation (1).

As in I, we premultiply equation (1) by $\exp(-i\boldsymbol{k}_1 \cdot \boldsymbol{\rho})\gamma(\boldsymbol{\rho})$, and integrate throughout the scatterer area and obtain

$$\int_S \exp(-i\boldsymbol{k}_1 \cdot \boldsymbol{\rho}) \gamma(\boldsymbol{\rho}) \boldsymbol{E}(\boldsymbol{\rho})\, d\boldsymbol{\rho}$$

$$= \hat{\boldsymbol{e}}_i U_1(\boldsymbol{k}_1, \boldsymbol{k}_i) + k_0^2 \int_S d\boldsymbol{\rho} \int_S d\boldsymbol{\rho}'\, \gamma(\boldsymbol{\rho}) \exp(-i\boldsymbol{k}_1 \cdot \boldsymbol{\rho})$$

$$\times \left(\mathbf{1} + \frac{1}{k_0^2} \nabla\nabla\right) g(\boldsymbol{\rho}, \boldsymbol{\rho}') \gamma(\boldsymbol{\rho}') \boldsymbol{E}(\boldsymbol{\rho}') \tag{11}$$

where

$$U_1(\boldsymbol{k}_1, \boldsymbol{k}_2) = \int_S \gamma(\boldsymbol{\rho}) \exp[i(\boldsymbol{k}_2 - \boldsymbol{k}_1) \cdot \boldsymbol{\rho}]\, d\boldsymbol{\rho} \tag{12}$$

and $\boldsymbol{k}_1$ is at present arbitrary.

Equation (5) may be treated similarly. This is an integral equation only involving the field inside the scatterer. As such, its solution is not unique in the external region. However, since we only need the solution in the internal region, we can assume that the solution of (11) is square integrable and hence may be written as

$$\boldsymbol{E}^{(H)}(\boldsymbol{\rho}) = \int \boldsymbol{C}^{(H)}(\boldsymbol{k}_2) \exp(i\boldsymbol{k}_2 \cdot \boldsymbol{\rho})\, d\boldsymbol{k}_2 \tag{13}$$

or

$$E^{(E)}(\boldsymbol{\rho}) = \int C^{(E)}(\boldsymbol{k}_2) \exp(i\boldsymbol{k}_2 \cdot \boldsymbol{\rho})\, d\boldsymbol{k}_2. \tag{14}$$

Substituting (12), (13) into (9) and its similar equation, we have:

(i) for the H wave

$$\int \mathbf{K}(\boldsymbol{k}_1, \boldsymbol{k}_2) \cdot \boldsymbol{C}^{(H)}(\boldsymbol{k}_2)\, d\boldsymbol{k}_2 = \hat{\boldsymbol{e}}_i U_1(\boldsymbol{k}_1, \boldsymbol{k}_i) \tag{15}$$

where

$$\mathbf{K}(\boldsymbol{k}_1, \boldsymbol{k}_2) = W(\boldsymbol{k}_1, \boldsymbol{k}_2)\mathbf{1} - \mathbf{U}_2^{(H)}(\boldsymbol{k}_1, \boldsymbol{k}_2)$$

$$\mathbf{U}_2^{(H)}(\boldsymbol{k}_1, \boldsymbol{k}_2) = \int\int \mathrm{d}\boldsymbol{\rho}\, \mathrm{d}\boldsymbol{\rho}'\, \gamma(\boldsymbol{\rho}) \exp(-\mathrm{i}\boldsymbol{k}_1 \cdot \boldsymbol{\rho})[\nabla_\rho \times (\nabla_\rho \times g(\boldsymbol{\rho}, \boldsymbol{\rho}')\mathbf{1})] \exp(\mathrm{i}\boldsymbol{k}_2 \cdot \boldsymbol{\rho}')\gamma(\boldsymbol{\rho}') \tag{16}$$

and

$$W(\boldsymbol{k}_1, \boldsymbol{k}_2) = \int_S \epsilon(\boldsymbol{\rho})\gamma(\boldsymbol{\rho}) \exp[\mathrm{i}(\boldsymbol{k}_2 - \boldsymbol{k}_1) \cdot \boldsymbol{\rho}]\, \mathrm{d}\boldsymbol{\rho}. \tag{17}$$

(ii) for the E wave

$$\int K(\boldsymbol{k}_1, \boldsymbol{k}_2) C^{(E)}(\boldsymbol{k}_2)\, \mathrm{d}\boldsymbol{k}_2 = U_1(\boldsymbol{k}_1, \boldsymbol{k}_i) \tag{18}$$

where $K(\boldsymbol{k}_1, \boldsymbol{k}_2) = U_1(\boldsymbol{k}_1, \boldsymbol{k}_2) - U_2^{(E)}(\boldsymbol{k}_1, \boldsymbol{k}_2)k_0^2$ and

$$U_2^{(E)}(\boldsymbol{k}_1, \boldsymbol{k}_2) = \int_S \int_S \mathrm{d}\boldsymbol{\rho}\, \mathrm{d}\boldsymbol{\rho}'\, \gamma(\boldsymbol{\rho}) \exp(-\mathrm{i}\boldsymbol{k}_1 \cdot \boldsymbol{\rho}) g(\boldsymbol{\rho}, \boldsymbol{\rho}') \exp(\mathrm{i}\boldsymbol{k}_2 \cdot \boldsymbol{\rho}')\gamma(\boldsymbol{\rho}'). \tag{19}$$

The corresponding scattering amplitudes become

$$f^{(H)}(\phi_s) = \lambda(\mathbf{1} - \hat{\boldsymbol{k}}_s\hat{\boldsymbol{k}}_s) \cdot \int \mathrm{d}\boldsymbol{k}_2\, \boldsymbol{C}^{(H)}(\boldsymbol{k}_2) U_1(\boldsymbol{k}_2, \boldsymbol{k}_s) \tag{20}$$

and

$$f^{(E)}(\phi_s) = \lambda \int \mathrm{d}\boldsymbol{k}_2\, C^{(E)}(\boldsymbol{k}_2) U_1(\boldsymbol{k}_2, \boldsymbol{k}_s). \tag{21}$$

Equations (15) and (20) (or (18) and (21)) are a pair of coupled integral equations which together determine the amplitude. Unlike equation (1), however, the kernel of (15) is not singular. We may therefore evaluate the integrations by N-point numerical quadrature. The integral equations then become algebraic linear equations, and the arbitrary vector $\boldsymbol{k}_1$ is restricted to N arbitrary values which we take to be the same as the pivots. Thus (15) and (20) are replaced by

$$\sum_{j=1}^{N} \mathbf{K}(\boldsymbol{k}_\rho, \boldsymbol{k}_j) \cdot \boldsymbol{C}^{(H)}(\boldsymbol{k}_j)\omega_j = \hat{\boldsymbol{e}}_i U_1(\boldsymbol{k}_\rho, \boldsymbol{k}_i) \qquad \rho = 1, \ldots, N \tag{22}$$

and

$$f^{(H)}(\phi_s) = \lambda(\mathbf{1} - \hat{\boldsymbol{k}}_s\hat{\boldsymbol{k}}_s) \cdot \sum_{j=1}^{N} \omega_j \boldsymbol{C}^{(H)}(\boldsymbol{k}_j) U_1(\boldsymbol{k}_j, \boldsymbol{k}_s). \tag{23}$$

Provided that for each $\boldsymbol{k}_j$ pivot, $-\boldsymbol{k}_j$ is also a pivot, then, as is shown in I, the Schwinger variational principle is automatically satisfied. This results in the method being numerically stable, and convergence with N being guaranteed.

3. Matrix elements for homogeneous elliptic cylinders

For a homogeneous scatterer where

$$\gamma(\boldsymbol{r}) \equiv n_0^2 - 1 = \text{constant} \tag{24}$$

an important simplification occurs. This is due to the fact that for a homogeneous scatterer the internal field of the scatterer can be represented as a superposition of plane waves with a radial variable $k_0 n_0$ (Devaney and Wolf 1974) and hence

$$\boldsymbol{C}^{(H)}(\boldsymbol{k}_2) = \delta(k - k_0 n_0)\boldsymbol{D}^{(H)}(\boldsymbol{k}_2) \tag{25}$$

where $\delta(k)$ is the Dirac delta function. Consequently the integrations in (15), (18), (20), (21) reduce to one-dimensional integrals.

We define the cross-sectional area S by the equation

$$\frac{x^2}{a^2} + \frac{y^2}{b^2} = 1. \tag{26}$$

In order to apply the method outlined in § 2 we need to be able to evaluate the matrices $\mathbf{K}$, U_1 in (22). The calculation of $U_1(\boldsymbol{k}_1, \boldsymbol{k}_2)$, the first Born term, is straightforward and we obtain

$$U_1(\boldsymbol{k}_1, \boldsymbol{k}_2) = 2\pi ab\gamma \frac{J_1(Z)}{Z} \tag{27}$$

where

$$Z = |\boldsymbol{K}_1 - \boldsymbol{K}_2| \tag{28}$$

$$\boldsymbol{K}_i = k_i(a\cos\phi_t, b\sin\phi_t); \qquad i = 1, 2, \tag{29}$$

and $J_n(x)$ denotes the Bessel function of order n. $W_1(\boldsymbol{k}_1, \boldsymbol{k}_2)$ is just a constant multiple of $U_1(\boldsymbol{k}_1, \boldsymbol{k}_2)$ for homogeneous scatterers.

In order to compute $U_2^{(E)}(\boldsymbol{k}_1, \boldsymbol{k}_2)$ we use the representation

$$g(\boldsymbol{\rho}, \boldsymbol{\rho}') = \frac{1}{4\pi^2} \lim_{\epsilon \to 0} \int_0^\infty \frac{t\,\mathrm{d}t}{t^2 - k_0^2 - \mathrm{i}\epsilon} \int_0^{2\pi} \mathrm{d}\phi_t \exp[\mathrm{i}(\boldsymbol{\rho} - \boldsymbol{\rho}') \cdot t]. \tag{30}$$

Substituting (30) into (19) and using (27) gives

$$U_2^{(E)}(\boldsymbol{k}_1, \boldsymbol{k}_2) = \gamma^2 a^2 b^2 \lim_{\epsilon \to 0+} \int_0^\infty \frac{t\,\mathrm{d}t}{t^2 - k_0^2 - \mathrm{i}\epsilon} \int_0^{2\pi} \mathrm{d}\phi_t \frac{J_1(X_1)J_1(X_2)}{X_1 X_2} \tag{31}$$

where

$$X_i = |\boldsymbol{T} - \boldsymbol{K}_i| \qquad (i = 1, 2) \tag{32}$$

and

$$\boldsymbol{T} = t(a\cos\phi_t, b\sin\phi_t). \tag{33}$$

Using the expansion (Watson 1966)

$$\frac{J_1(X_j)}{X_j} = 2 \sum_{m=0}^{\infty} (m+1) \frac{J_{m+1}(T)J_{m+1}(K_j)}{TK_j} C_m^1(\hat{\boldsymbol{T}} \cdot \hat{\boldsymbol{K}}_j) \tag{34}$$

(where $C_m^1(x)$ is a Gegenbauer polynomial) and the integrals (Watson 1966)

$$\lim_{\epsilon \to 0+} \int_0^\infty \frac{tJ_m(tY)J_n(tY)}{t^2 - k_0^2 - \mathrm{i}\epsilon} \mathrm{d}t = \frac{\pi \mathrm{i}}{2} H_{m<}^{(1)}(k_0 Y) J_{m>}(k_0 Y) \tag{35}$$

$$\int_0^\infty \frac{J_m(tY)J_n(tY)}{t} \mathrm{d}t = \frac{2}{\pi n} \delta_{nm} \tag{36}$$

where

$$m_> = \max(n, m) \qquad m_< = \min(n, m) \tag{37}$$

and δ_{nm} is the Kronecker delta, we finally obtain

$$U_2^{(E)}(\boldsymbol{k}_1, \boldsymbol{k}_2) = \frac{4a^2b^2\pi\gamma^2}{k_0^2} \int_0^{\pi} \frac{\mathrm{d}\phi_t}{Y^2} \sum_{\substack{nm \\ n+m \\ \text{even}}}\sum (n+1)(m+1)\frac{J_{n+1}(K_1)}{K_1}\frac{J_{m+1}(K_2)}{K_2}$$

$$\times C_n^1(\hat{\boldsymbol{K}}_1 \cdot \hat{\boldsymbol{T}}) C_m^1(\hat{\boldsymbol{K}}_2 \cdot \hat{\boldsymbol{T}}) \left(\mathrm{i} H_{m_<+1}(k_0 Y) J_{m_>+1}(k_0 Y) - \frac{\delta_{nm}}{\pi(n+1)} \right) \tag{38}$$

where

$$Y^2 = a^2 \cos^2 \phi + b^2 \sin^2 \phi. \tag{39}$$

The evaluation of $\mathbf{U}_2^{(H)}(\boldsymbol{k}_1, \boldsymbol{k}_2)$ is similar and the result is

$$\mathbf{U}_2^{(H)}(\boldsymbol{k}_1, \boldsymbol{k}_2) = 4a^2b^2\pi\gamma^2 \int_0^{\pi} \mathrm{d}\phi_t (\mathbf{1} - \hat{\hat{\boldsymbol{t}}\boldsymbol{t}}) \sum_{\substack{n=0 \\ n+m \text{even}}}^{\infty} \sum_{m=0}^{\infty} (m+1)(n+1)\frac{J_{n+1}(K_1)}{K_1}\frac{J_{m+1}(K_2)}{K_2}$$

$$\times \mathrm{i} J_{m_>+1}(k_0 Y) C_n^1(\hat{\boldsymbol{K}}_1 \cdot \hat{\boldsymbol{T}}) C_m(\hat{\boldsymbol{K}}_2 \cdot \hat{\boldsymbol{T}}) H_{m_<+1}(k_0 Y) \tag{40}$$

where

$$\mathbf{1} - \hat{\hat{\boldsymbol{t}}\boldsymbol{t}} = \begin{pmatrix} \sin^2 \phi_t & -\sin \phi_t \cos \phi_t \\ -\sin \phi_t \cos \phi_t & \cos^2 \phi_t \end{pmatrix}. \tag{41}$$

4. Numerical results

4.1. Elliptic cross section infinite cylinders

Numerical computation has been performed for elliptic cross section scatterers for E- and H-wave cases. Since for homogeneous scatterers quadrature points are required only for ϕ, we use n_ϕ equally spaced ϕ pivots. The matrix size of equation (22) is minimized using the symmetry and reciprocity properties of the matrix elements. The program is written in double precision and tested against the exact solution for circular cylinders with which an excellent agreement has been obtained.

For elliptic cross section scatterers the accuracy of the results was ensured by increasing n_ϕ and observing the convergence of the results. The number of pivots required to obtain convergence depends on the size, shape and refractive index of the scatterer. In table 1 a sample convergence pattern is given.

In order to describe the depolarizing properties of the cylindrical scatterers it is essential to know the forward and backward scattering amplitudes. In tables 2, 3 complex scattering amplitudes are presented for a range of a/b ratios. The total cross section σ can be obtained by the optical theorem as

$$\sigma = -2(\pi/k_0)^{1/2} \operatorname{Re}[(1+\mathrm{i})f(0)].$$

The variation of the scattered wave intensity and phase is shown in figure 1 for two scatterers. For elliptical cylinders the intensity functions have more maxima and

Table 1. Convergence of the forward scattering amplitude for scattering of an incident E wave, $\phi_i = 0$, $k_0 = 1$ by an infinite elliptic cylinder of dielectric $\epsilon(\rho) = 2{\cdot}0$ and semi-axes $a = 3\pi/2$, $b = \pi$.

n_ϕ	$f^{(E)}(0)$
5	−4·4287+i3·9122
6	−4·6007+i3·9652
7	−4·5928+i3·9708
8	−4·5921+i3·9713
9	−4·5918+i3·9698

Table 2. Forward and backward scattering amplitudes for scattering of an incident E wave, $k_0 = 1$ by infinite elliptic cylinders of dielectric $\epsilon(\rho) = 2{\cdot}0$ and $b = \pi$.

a/b	ϕ_i	$f^{(E)}(0)$	$f^{(E)}(\pi)$
1·0	0	−1·568+i4·381	−0·875−i0·330
1·2	0	−2·964+i4·495	−0·450−i0·426
1·4	0	−3·911+i4·172	0·649+i0·727
1·6	0	−5·12 +i3·38	−0·529+i0·138
2·0	0	−5·71 +i1·17	−0·158+i0·808
1·2	$\pi/2$	−1·928+i5·008	−0·504−i0·586
1·4	$\pi/2$	−2·040+i5·557	−0·156−i0·330
1·6	$\pi/2$	−2·28 +i6·30	−0·354+i0·131
2·0	$\pi/2$	−2·40 +i7·81	−1·074−i0·230

Table 3. Forward and backward scattering amplitudes for scattering of an incident H wave, $k_0 = 1$ by infinite elliptic cylinders of dielectric $\epsilon(\rho) = 2{\cdot}0$, and $b = \pi$.

a/b	ϕ_i	$f^{(H)}(0)$	$f^{(H)}(\pi)$
1·0	0	−0·969+i4·234	−0·383+i0·0017
1·2	0	−2·057+i4·550	0·161+i0·016
1·4	0	−3·113+i4·369	0·265+i0·442
1·6	0	−4·17 +i3·89	0·330−i0·077
2·0	0	−5·09 +i1·94	0·021+i1·26
1·2	$\pi/2$	−1·253+i4·889	−0·455+i0·081
1·4	$\pi/2$	−1·485+i5·560	−0·676+i0·076
1·6	$\pi/2$	−1·72 +i6·24	−0·830−i0·097
2·0	$\pi/2$	−2·27 +i7·67	−0·580−i0·225

minima in comparison with a circular scatterer of the same geometrical cross section. This is due to the excitation of higher-order partial waves inside the non-circular scatterer. In essence this property can be used in the determination of a/b ratios from measurement results.

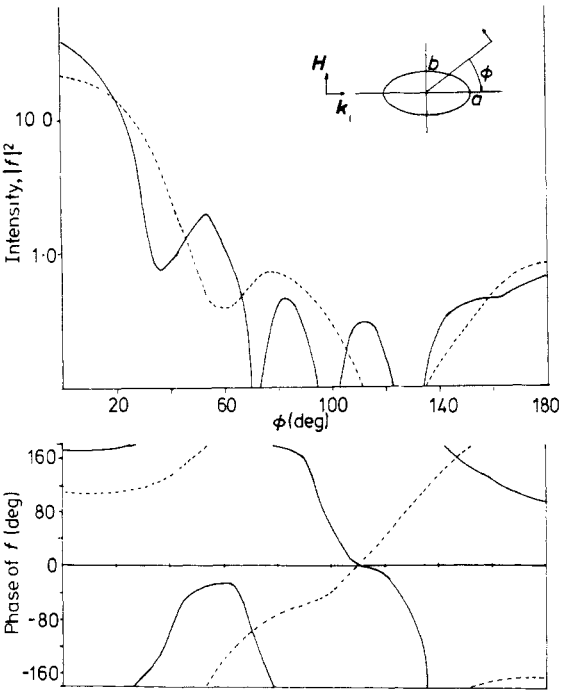

Figure 1. Scattered wave intensity and phase against observation angle ϕ. Full curves, $a/b = 2{\cdot}0$; broken curves, $a/b = 1{\cdot}0$, E-wave case.

Comparison has been made with results published by Nelson and Eyges (1976) and a good agreement has been obtained. Nelson and Eyges (1976) commented that their results showed a substantial deviation from those of Yeh (1965), even for $a/b \sim 1$. We find our results for the intensity in the backward direction differ significantly from those of Yeh (1965), but agree with those of Nelson and Eyges (1976).

4.2. Three-dimensional scatterers

Numerical results have been obtained using the same method for three-dimensional scatterers. The details of the analysis for this case have been given elsewhere (Holt *et al* 1976a). The scattered field is defined by the relation

$$\boldsymbol{E}(\boldsymbol{r}) \underset{r\to\infty}{\sim} \hat{\boldsymbol{e}}_i\, e^{i\boldsymbol{k}_i\cdot\boldsymbol{r}} + \boldsymbol{f}(\boldsymbol{k}_s, \boldsymbol{k}_i, \hat{\boldsymbol{e}}_i)\frac{e^{ik_0 r}}{r} \tag{42}$$

where $\hat{\boldsymbol{e}}_i\, e^{i\boldsymbol{k}_i\cdot\boldsymbol{r}}$ is the incident wave, and $\boldsymbol{f}(\boldsymbol{k}_s, \boldsymbol{k}_i, \hat{\boldsymbol{e}}_i)$ is the scattering amplitude at the observation direction $\boldsymbol{k}_s$.

Numerical calculations have been performed for spheroids defined by the equation

$$\frac{x^2+y^2}{a^2}+\frac{z^2}{b^2}=1 \tag{43}$$

as shown in figure 2. The most important difference in scattering from spheroidal scatterers compared to that from spherical scatterers is the depolarizing properties caused by the non-sphericity when $\hat{\boldsymbol{k}}_i \neq \hat{\boldsymbol{z}}$. The depolarization occurs because for an

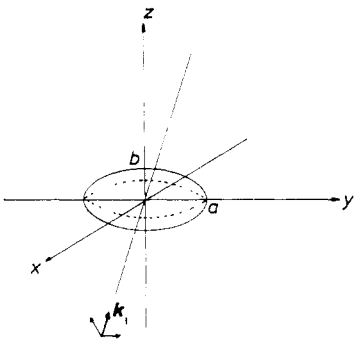

Figure 2. Scattering geometry for a spheroidal scatterer.

arbitrary $\hat{\boldsymbol{k}}_i(\neq\hat{\boldsymbol{z}})$ the two independent polarizations have different scattering amplitudes, this difference increases as the incident wavevector $\boldsymbol{k}_i$ approaches the x–y plane. In table 4 numerical results are given for several scatterers and three independent incident waves, corresponding to principal axes of the spheroids, the refractive index is $n_0=\sqrt{\epsilon}=1{\cdot}33$.

We define the intensity function

$$i(\theta)=|f(\boldsymbol{k}_s;\boldsymbol{k}_i,\hat{\boldsymbol{e}}_i)|^2 \tag{44}$$

to be $i_1(\theta)$ in the plane $\hat{\boldsymbol{k}}_s\cdot\hat{\boldsymbol{y}}=0$ and to be $i_2(\theta)$ in the plane $\hat{\boldsymbol{k}}_s\cdot\hat{\boldsymbol{x}}=0$, when $\hat{\boldsymbol{k}}_i=\hat{\boldsymbol{z}}$, where we define

$$\cos\theta=\hat{\boldsymbol{k}}_i\cdot\hat{\boldsymbol{z}}. \tag{45}$$

In figures 3, 4, 5, we give $i_1(\theta)$, $i_2(\theta)$ for four different scatterers. For small scatterers the patterns are similar to those for scatterers in the Rayleigh region. As the scatterer size increases $i_1(\theta)$, $i_2(\theta)$ are more oscillatory due to interference effects between the higher-order partial waves. Just as for spherical scatterers, when the scatterer is large almost all the scattered energy is in the forward direction.

We have also performed calculations to compare with those of Asano and Yamamoto (1975) and have obtained good agreement (see Holt *et al* 1976b).

Table 4. Forward scattering amplitudes for a range of spheroidal scatterers with $a/b=2{\cdot}0$ (oblate) and $a/b=0{\cdot}5$ (prolate); $n_0=1{\cdot}33$.

a	b	$f(k_0\hat{\boldsymbol{z}},k_0\hat{\boldsymbol{z}},\hat{\boldsymbol{x}})$	$f(k_0\hat{\boldsymbol{x}},k_0\hat{\boldsymbol{x}},\hat{\boldsymbol{z}})$	$f(k_0\hat{\boldsymbol{x}},k_0\hat{\boldsymbol{x}},\hat{\boldsymbol{y}})$
1·0	0·5	0·118+i0·00767	0·0979+i0·00441	0·119 +i0·00679
2·0	1·0	0·896+i0·270	0·857 +i0·154	1·033 +i0·265
3·0	1·5	2·79 +i1·02	2·94 +i1·30	3·19 +i1·88
4·0	2·0	6·23 +i3·54	5·92 +i4·88	5·84 +i6·05
5·0	2·5	10·8 +i7·46	8·71 +i11·7	8·33 +i13·2
6·50	3·25	19·0 +i19·9	6·8 +i27·5	6·3 +i30·1
0·5	1·0	0·0515+i0·00130	0·0604+i0·00214	0·0512+i0·00148
1·0	2·0	0·456 +i0·056	0·507 +i0·108	0·426 +i0·065
1·5	3·0	1·67 +i0·545	1·56 +i0·588	1·42 +i0·354
2·0	4·0	3·74 +i2·44	3·47 +i1·84	3·38 +i1·39
2·5	5·0	5·64 +i6·59	6·00 +i4·27	5·86 +i3·46
3·25	6·50	4·4 +i16·4	10·6 +i11·0	10·8 +i9·9

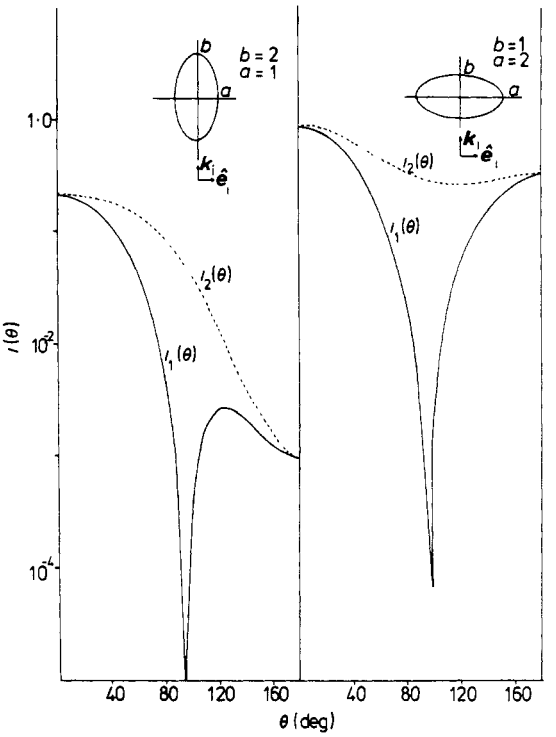

Figure 3. $i_1(\theta)$, $i_2(\theta)$ intensity functions for two spheroids $k_0 = 1$, $\sqrt{\epsilon} = 1{\cdot}33$.

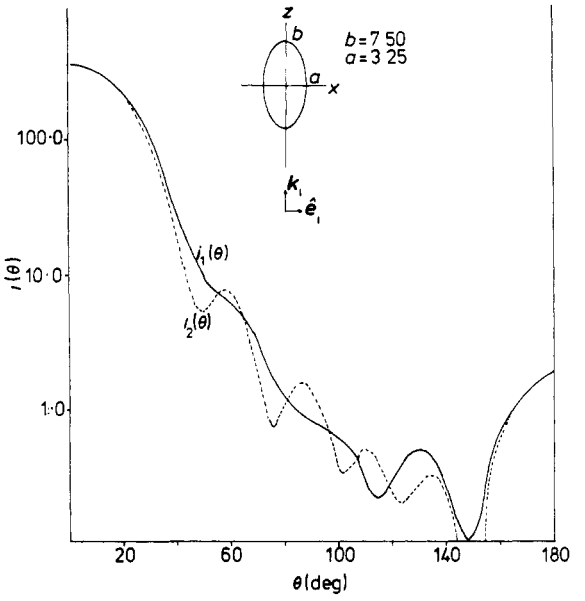

Figure 4. $i_1(\theta)$, $i_2(\theta)$ intensity functions for a prolate spheroidal scatterer, $k_0 = 1$, $\sqrt{\epsilon} = 1{\cdot}33$.

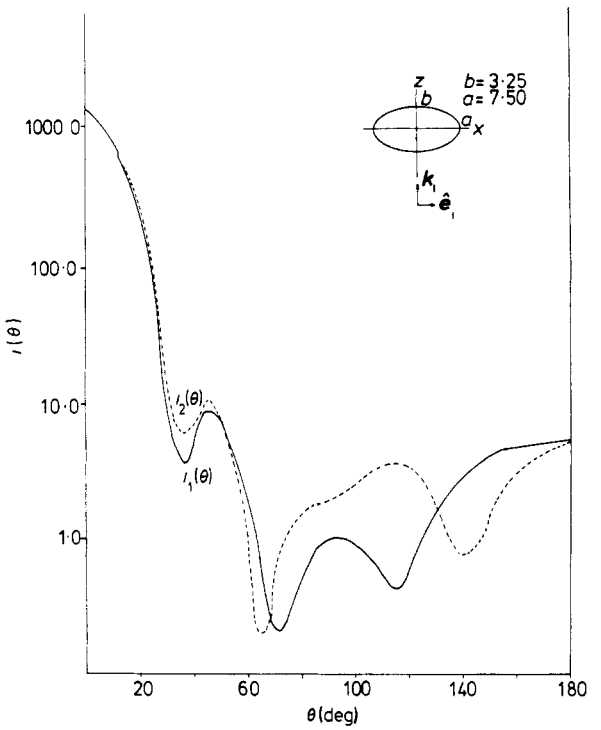

Figure 5. $i_1(\theta)$, $i_2(\theta)$ intensity functions for an oblate spheroidal scatterer, $k_0 = 1$, $\sqrt{\epsilon} = 1{\cdot}33$.

5. Conclusion

The method we have developed has been shown to be very suitable for obtaining the scattering amplitude for the scattering of electromagnetic radiation by homogeneous dielectric scatterers. For the optical case, we have obtained results for infinite elliptic cylinders, for spheroids and for ellipsoids (Holt *et al* 1976b). Moreover it has been shown to be applicable to a very wide range of scatterers—from those in the Rayleigh region even up to the geometrical optics limit. The limitation is that certain matrix elements must be capable of being evaluated. Given this constraint, it should be possible to deal with inhomogeneous dielectrics and/or other shapes of scatterer.

Acknowledgments

This work was supported in part by a grant from the Science Research Council, to whom our thanks are due. All the calculations were performed on the PDP-10 installation at the University of Essex.

References

Asano S and Yamamoto G 1975 *Appl. Opt.* **14** 29
Barber P and Yeh C 1975 *Appl. Opt.* **14** 2864

Devaney A J and Wolf E 1974 *J. Math. Phys.* **75** 234–44
Gans R 1912 *Ann. Phys., Lpz.* **37** 881
Holt A R, Uzunoglu N K and Evans B C 1976a *IEEE Trans. Antennas Propag.* submitted for publication
—— 1976b *Abstracts 1976, Int. IEEE/AP-S Symp.* (New York: IEEE)
Ignatowsky V W 1905 *Ann. Phys., Lpz.* **23** 495
Mie G 1908 *Ann. Phys., Lpz.* **25** 377
Nelson A and Eyges L 1976 *J. Opt. Soc. Am.* **66** 254
Rayleigh L 1881 *Phil. Mag.* **12** 81
—— 1899 *Phil. Mag.* **47** 375
Stevenson A F 1953 *J. Appl. Phys.* **24** 1134
Uzunoglu N K, Evans B G and Holt A R 1976a *Electron. Lett.* **12** 312–3
—— 1976b *Proc. IEE* submitted for publication
Waterman P C 1965 *Proc. IEEE* **53** 805
Watson G N 1966 *The Theory of Bessel Functions* 2nd edn (Cambridge: Cambridge University Press)
Yeh C 1965 *J. Opt. Soc.* **55** 309–14